

PAPER • OPEN ACCESS

Identification of subsurface layer in UNNES reservoir basin

To cite this article: S Supriyadi *et al* 2020 *J. Phys.: Conf. Ser.* **1567** 022005

View the [article online](#) for updates and enhancements.

You may also like

- [Correlation between Resistivity and Ground Penetrating Radar \(GPR\) Methods in Understanding the Signatures in Detecting Cavities](#)
Muhamad Afiq Saharudin, Umi Maslinda, Hazrul Hisham et al.
- [Electrical resistivity interpretation of ternary Cu–Ni–Mo alloys using a cluster-based short-range-order structural model](#)
Hongming Li, Yajun Zhao, Xiaona Li et al.
- [Depth estimation of the aquifer layer using the geoelectric resistivity method](#)
F D Sastrawan, Asrafil and E G Prasetya



ECS The Electrochemical Society
Advancing solid state & electrochemical science & technology

243rd Meeting with SOFC-XVIII

Boston, MA • May 28 – June 2, 2023

Accelerate scientific discovery!

Learn More & Register

Identification of subsurface layer in UNNES reservoir basin

S Supriyadi*, K Khumaedi, T M Mukromin, M Yani and F Setiawan

Department of Physics, Faculty of Mathematics and Natural Sciences, Universitas Negeri Semarang, Indonesia

*Corresponding author: supriyadi@mail.unnes.ac.id

Abstract. Reservoir basin is one of the important components in water conservation which is very supportive in Green Campus activities. The importance of information on the sub-surface layer surrounding the reservoir basin is the first step in managing and empowering the location. The purpose of this research is to identify the subsurface layers in the UNNES reservoir basin. The method used in this research is the resistivity geoelectric method with the Wenner configuration. Measured track totaling three which is located on the side of the UNNES reservoir basin with a track length of 75 m. The results of the identification of the subsurface layer get four layers, namely the layer of tuff sand/water with a value of 1.22 - 2.79 Ωm , a layer of clay with a value of 6.41 - 14.7 Ωm , a layer of sand / gravel with a value of 33, 7 - 77.3 Ωm and lava flow / breccia flow with a value of 77.4 - 177 Ωm .

1. Introduction

An appropriate approach to estimating reservoir benefits must recognize reservoirs as assets that provide services across many years (for example, flood control, recreational area, good aesthetic view, power generation energy). The function reservoir for level sediment is increasing marginal in sediment [1]. Rock foundation is needed to support the carrying capacity of rocks like geological and structural factors. Information about the subsurface structure is very important in determining the strength of the foundation stone bearings [2]. To understand how the mechanism that occurs under the surface, must understand first internal structure. Because getting insight about this indirect structure, usually a single example be investigated [3]. UNNES reservoir basin actively supports one activity as a green campus in UNNES, so it is essential to investigate to find out the subsurface condition to be able to maintain further.

A Geophysical investigations provide a fast and cost-effective way for developing information about subsurface [4]. Geophysical investigation involving the electrical resistivity method was, therefore, carried out to delineate the geoelectric layer and their geoelectric parameters, mapping the soil corrosivity and identifying possible geologic structures such as fractures [5].

In investigating underground surfaces, a method called geoelectrical resistivity is needed. One of the components in this method is that rocks have a role, including potential and currents below the earth's surface. The good results require a combination measurement like direct resistivity and subsurface [6]. Direct current resistivity is the method most often used [7]. The electrical resistivity method is a useful geophysical tool in the evaluation of the dam because it is sensitive to changes in lithology, water saturation, and water chemistry [8]. Changes that occur in underground resistivity can be known by using a geoelectric monitoring survey. The measurement is repeated several times using the same distance electrode [9].



Geoelectrical measurements obtain information on structural resistivity on the ground by recording the electric potential that arises from currents enter the ground. The current flowing out from the source with revealing the equipotential surface and moving perpendicular to the current flow, then forming a semicircle, is called the homogeneous position of the soil. In situations that usually occur, the current source, current sink, current flow, and equipotential become more complex. Current flow and equipotential can be very complex due to changes in resistivity [10].

MN electrodes have the potential difference caused by AB electrodes due to current injection, and the formula is as follows:

$$\Delta V = V_M - V_N \tag{1}$$

Another name for geoelectrical data is usually mentioned with apparent resistivity

$$\rho = \frac{\Delta V}{I} k \tag{2}$$

The commonly used method in resistivity, as shown in Figure 1.

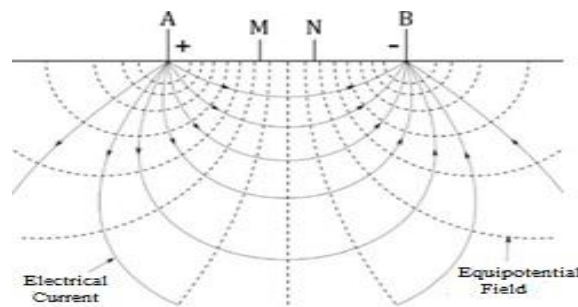


Figure 1. Equipotential surface and direction of electric current due to two current sources (I and - I) on a homogeneous earth surface.

The information obtained in the 2D imaging survey follows through by a computer that controls the resistivity device connected to the multi-electrode system. The automatic software control will select four electrodes for each measurement to give a 2D image of the underground surface [11].

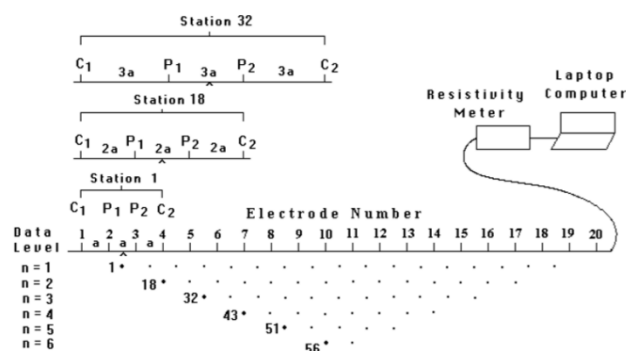


Figure 2. 2D electrode arrangement of electrical survey and measurement methods Wenner to obtain pseudo section

Figure 2 represents the measurement rules for the Wenner electrode method used in this study. The space used between the electrodes is “a.” For the first measurement, electrodes 1, 2, 3, and 4 have been used. Electrode 1 is used as the primary current of electrode C1, electrode 2 as the first potential of electrode P1, electrode 3 as the second potential of electrode P2, and electrode 4 as the second potential of electrode C2. In the second measurement, the electrodes used were electrodes 2, 3, 4, and 5, which were used for the roles of C1, P1, P2, and C2. Repetition continues up to the electrodes to 31, 32, 33, and 34 until the last measurement with space “1a” space. After finishing with the space “1a” then proceed with the space “2a”. The first measurement used electrodes in the order of 1, 3, 5, and 7. The second measurement used electrodes order is 2, 4, 6, and 8. This process will repeat until the electrodes 28, 30, 32, and 34 with spaces “2a”. Use the same process with measurements “3a”, “4a”, “5a,” and “6a” spaces [11]. Wenner configuration has benefit in a much deeper penetration, strong stability, and detect images both vertically and horizontally below the surface. Each setting has benefit and detriment [12].

2. Methods

This research was conducted at the edge of the reservoir of Semarang State University to determine the subsurface structure of the local location. The location only took 3 lines flanking the site in representing the survey location of the reservoir area. The research location explained in Figure 3.



Figure 3. Research locations on the side of the UNNES reservoir basin.

The method used is resistivity by mapping or horizontally. Electromagnetic induction and producing contour map of apparent cause by interpolation are some way this method measurement to conductivity subsurface [13]. The configuration used is the Wenner configuration because the Wenner configuration has advantages in the accuracy of the reading with the eccentricity value is not large, that is worth 1/3. Besides that, the Wenner configuration is a configuration that has a good signal compared to other settings. Wenner-Schlumberger array gives a significant median depth of investigation and excellent presentation for the subsurface both in horizontal and vertical coverage with more details [14]. The tool used in this study is Bawono-Georesist Resistivitymeter 12 GM-INV with 5 meters of spacing and a distance of 75 meters in each of its trajectories. The data obtained in the survey are electric current (I) and potential difference (ΔV). An inverted model can be made with topographic information, which recorded data elevation use handheld GPS for each electrode location [15].

Furthermore, pseudo resistivity values are obtained through data processing using Ms. Excel and data interpretation using Res2divn software to display 2D cross-sections and Voxler software to display 3D shapes. In the quantitative interpretation method, real resistivity and thickness of bellow the surface layers are obtained. The main objective of this interpretation method is to get the

geoelectrical parameters and parts. Regularly to gain more knowledge about the subsurface geology of the area, each line is represented [16].

3. Results and Discussion

Results of the 2D pseudo section cross section-analysis on lines 1, 2, and 3 are shown as follows.

- Line 1

Line 1 is located at coordinates 7°02'54.85" South latitude - 110°23'39.60" East longitude. Cross-section of 2D subsurface resistivity on line 1 with 5 iterations and root mean square (RMS) = 9.4% can be seen in Figure 4.

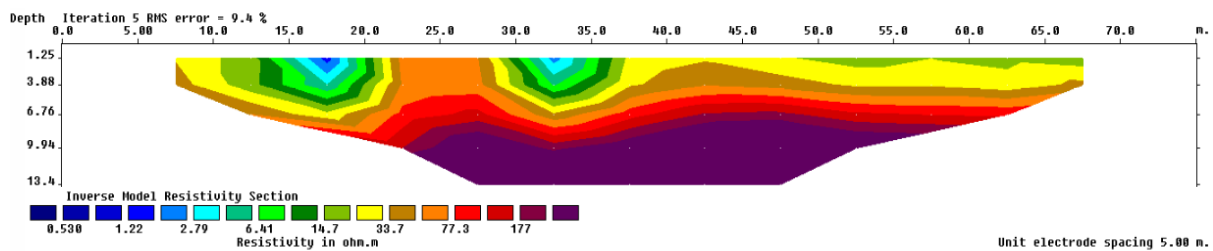


Figure 4. Cross-section resistance of sub-surface, line 1.

Based on Figure 4, there are 4 layers, namely tuff and sand layers, clay layer, sand/gravel layer, and lava flow/breccia layer. Layers of sand and tuff are shown at points 15-20 with depths of 0-3.88 meters and points 30-35 with depths of 0-2 meters. The clay layer is shown at locations 7-22 with a depth of 0-6.76 meters and points 28-75 with a depth of 0-6 meters. The sand and gravel layer is shown at points 22-28 with a depth of 0-8 meters and is located just below the horizontal clay layer. In comparison, the lava/breccia flow layer is shown with a depth of 6-13.4 meters and is located under the sand and gravel layer. The subsurface structure inline 1 on one side of the dam explained in Table 1.

Table 1. Subsurface structure, line 1.

Resistivity (Ωm)	Layer Type	Color Image
1,22 – 2,79	Tufan Sand and Water	Blue – Light Blue
6,41 – 14,7	Clay	Green – Yellowish Green
33,7 – 77,3	Sand and Gravel	Yellow – Orange
77,4 – 177	Lava Flow/Breccia	Red – Black

- Line 2

Line 2 is located at coordinates 7°02'53.04" South latitude - 110°23'41.62" East longitude. Cross-section of 2D subsurface resistivity on line 2 with 5 iterations and root mean square (RMS) = 18.5% can be seen in Figure 5.

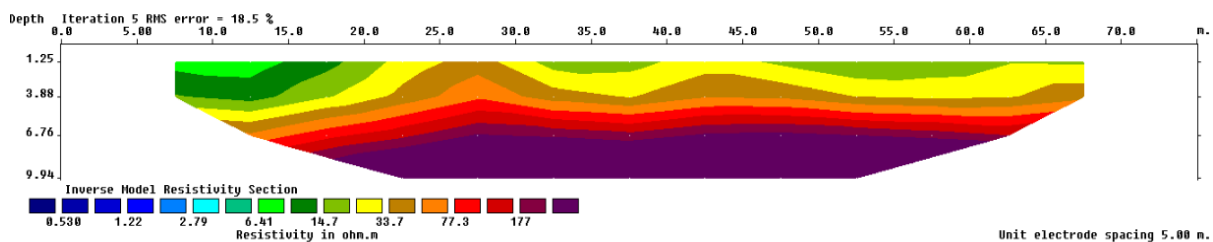


Figure 5. Cross-section resistance of sub-surface, line 2.

Based on Figure 5, there are 3 layers, namely clay layer, sand/gravel layer, and lava flow/breccia layer. The clay layer is shown at point 0-22 with a depth of 0-5 meters, point 32-40 with a depth of 0-2 meters, and point 46-68 with a depth of 0-3 meters. The sand and gravel layer is shown at point 22-32 with a depth of 0-7 meters and point 40-46 with a depth of 0-7 meters and is located just below the horizontal clay layer. In comparison, the thickness of lava/breccia flow is indicated by a depth of 5-9.94 meters and is located under a layer of sand and gravel. The subsurface structure of line 2 on one side of the dam can be seen in Table 2.

Table 2. Subsurface structure, line 2.

Resistivity (Ωm)	Layer Type	Color Image
6,41 – 14,7	Clay	Green – Yellowish Green
33,7 – 77,3	Sand and Gravel	Yellow – Orange
77,3 – 177	Lava Flow/Breccia	Red – Black

- Line 3

Line 3 is located at coordinates $7^{\circ}02'54.7''$ South latitude - $110^{\circ}23'41.88''$ East longitude. Cross-section of 2D subsurface resistivity on line 3 with 5 iterations and root mean square (RMS) = 9% can be seen in Figure 6.

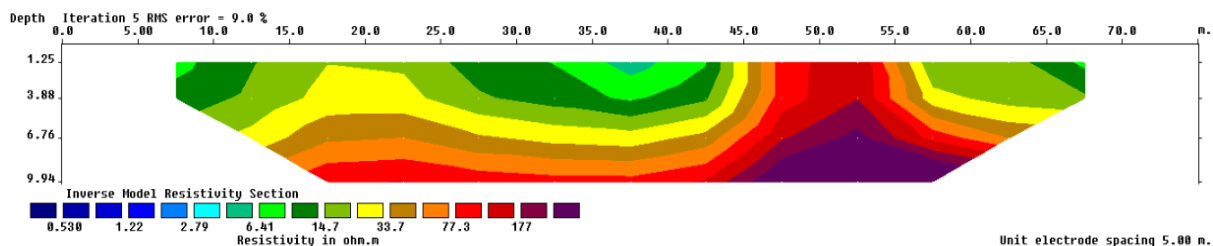


Figure 6. Cross-section resistance of sub-surface, line 3.

Based on Figure 6, there are 3 layers, namely clay layer, sand and gravel layer, and lava flow/breccia layer. The clay layer is shown at point 0-44 with a depth of 0-6.76 meters and point 57-75 with a depth of 0-5 meters. The sand and gravel layer is shown at point 44-47 with a depth of 0-9 meters and lead 54-57 with a depth of 0-7 meters, while the lava/breccia flow layer is shown at point 47-54 with a depth of 0-9.94 meters. The subsurface structure inline 3 on one side of the dam can be seen in Table 3.

Table 3. Subsurface structure, line 3.

Resistivity (Ωm)	Layer Type	Color Image
6,41 – 14,7	Clay	Green – Yellowish Green
33,7 – 77,3	Sand and Gravel	Yellow – Orange
77,3 – 177	Lava Flow/Breccia	Red – Black

Visualization of subsurface structures is critical to make it easier to see images that are below the surface, so they need a 3D appearance through the help of Voxler software. The results of the 3D visualization of subsurface structures can be seen in Figure 7.

Based on Figure 7 the resistivity values range from $2.7 \Omega\text{m}$ - $177 \Omega\text{m}$, seen as a whole the most abundant layer is the sand and gravel layer symbolized by a green color image. While the clay layer symbolized by blue color is only on the upper surface on each side of the track in very minimal

quantities. Figure 7 (b) shows that the lava layer/breccia symbolized by the yellow-red color image is seen on the surface at lane 3, this is very different from the lane 1 or lane 2 in Figure 7 (a) which is at the bottom of the surface.

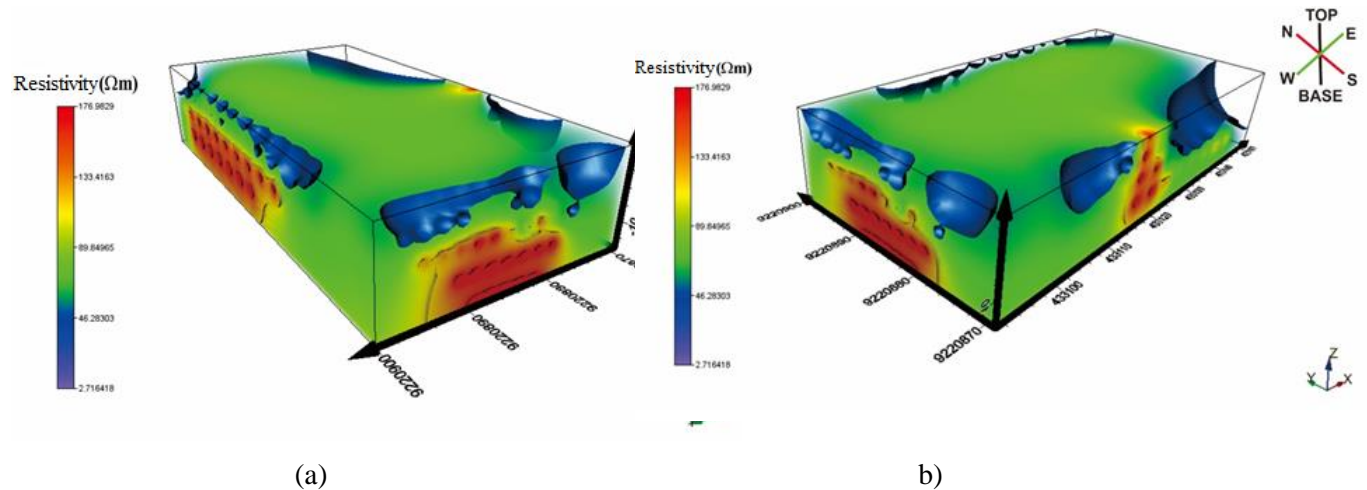


Figure 7. 3D Visualization of subsurface structures, (a) left side position, (b) right side position

4. Conclusion

The subsurface structure in the study area obtained 4 layers, namely tuff/sand (6.41 - 14.7 Ωm), clay (6.41 - 14.7 Ωm), sand/gravel (33.7 - 77.3 Ωm) and lava flow/breccias (77.3 - 177 Ωm) which are found on each lane on the edge/side of the UNNES reservoir basin.

References

- [1] Han Y, Feng G and Ouyang Y 2018 *Water* **10** 1333
- [2] Osinowo O O and Falufosi M O 2018 *NRIAG J. Astr. Geophys* **7** 309
- [3] Kasprzak M 2015 *Polar Research* **34** 1
- [4] Helaly A S 2017 *NRIAG J. Astr. Geophys* **6** 408
- [5] Ibitoye F P, Ojo J S, Akintorinwa O J, Olorunfemi M O, Adepelumi A A, Akinluwade K J, Taiwo A T, Isadare D A and Adentuji A R 2013 *J. App. Geol. Geophys.* **1** 46
- [6] Islami N 2019 *J. of Phys.: Conf. Ser.* **1185** 012027.
- [7] Kieu D T and Truong T C 2019 *ASEG Extended Abstracts* **1** 1
- [8] Fatoba O J, Eluwole A., Ademilua O L and Sanuade O A 2018 *Indian J. of Geosci.* **72** 275.
- [9] Loke M H, Wilkinson P B and Chambers J E 2016 *ASEG Extended Abstracts* **1** 1
- [10] Jamaluddin and Umar E P 2018 *J. Earth and Environ. Sci.* **118** 012006
- [11] Abdullahi N K and Baba G I 2017 *Sci. World J.* **12** 22.
- [12] Metwaly M and Alfouzan F 2013 *Geosci. Frontiers* **4** 469.
- [13] Dotta G, Gigli G, Ferrigno F, Gabbani G, Nocentini M, Lombardi L, Agostini A, Nolesini T and Casagni N 2017 *J. Rock Mech. and Rock Eng.* **50** 2397.
- [14] Solomon E O and Ogah V A 2019 *Sci. Res. J.* **7** 1
- [15] Anita D, Israil M, Anbalagan R and Gupta P K 2017 *J. App. Geophys.* **144** 78
- [16] Moghaddam S, Rouhani A K and Amiri A A 2017 *Iranian J. of Geophys.* **10** 22.